29-6-2007

Effect of confining pressure on ballast degradation and deformation under cyclic triaxial loading

J. Lackenby
University of Wollongong, jl40@uow.edu.au

Buddhima Indraratna
University of Wollongong, indra@uow.edu.au

G. McDowell
University of Nottingham, UK

D. Christie
RailCorp, Australia

Lackenby, J. *et al.* (2007). *Géotechnique* **57**, No. 6, 527–536 **doi:** 10.1680/geot.2007.57.6.527

Effect of confining pressure on ballast degradation and deformation under cyclic triaxial loading

J. LACKENBY*, B. INDRARATNA†, G. McDOWELL‡ and D. CHRISTIE§

Traditional railway foundations or substructures have become increasingly overloaded in recent years, owing to the introduction of faster and heavier trains. A lack of substructure re-engineering has resulted in maintenance cycles becoming more frequent and increasingly expensive. Two significant problems arising from increasing axle loads are differential track settlement and ballast degradation. One potential method of enhancing the substructure is to manipulate the level of ballast confinement. To investigate this possibility, a series of high-frequency cyclic triaxial tests has been conducted to examine the effects of confining pressure and deviator stress magnitude on ballast deformation (permanent and resilient) and degradation. Experimental results indicate that, for each deviator stress considered, an 'optimum' range of confining pressures exists such that degradation is minimised. This range was found to vary from 15–65 kPa for a maximum deviator stress of 230 kPa to 50–140 kPa when deviatoric stresses increase to 750 kPa. Ballast specimens tested at low confining pressures indicative of current in situ conditions were characterised by excessive axial deformations, volumetric dilation, and an unacceptable degree of degradation associated mainly with angular corner breakage. The results suggest that in situ lateral pressures should be increased to counteract the axle loads of heavier trains, and practical methods of achieving increased confinement are suggested.

KEYWORDS: deformation; gravels; laboratory tests; particle crushing/crushability; repeated loading

Les fondations ou infrastructures ferroviaires traditionnelles connaissent ces dernières années une surcharge croissante, en raison de l'introduction de trains plus lourds et plus rapides. Un manque de réingénierie des infrastructures a conduit à une augmentation de la fréquence et des coûts des cycles de maintenance. Le tassement différentiels des voies et la détérioration du ballast, provoqués par des charges par essieu croissantes, constituent deux problèmes importants. L'une des méthodes d'amélioration de l'infrastructure potentielle consisterait à manipuler le niveau de confinement du ballast. Pour étudier cette possibilité, une série de tests cycliques triaxiaux à haute fréquence a été réalisée pour examiner les effets de la pression de confinement et de l'amplitude de la contrainte déviatorique sur la dégradation et la déformation du ballast (permanente et résistante). Les résultats expérimentaux indiquent que, pour chaque contrainte déviatorique considérée, il existe une plage de pressions de confinement optimale telle que la détérioration soit minimale. La plage observée varie de 15-65 kPa pour une contrainte déviatorique maximale de 230 kPa jusqu'à 50-140 kPa lorsque les contraintes déviatoriques atteignent 750 kPa. Les échantillons de ballast testés à des pressions de confinement faibles correspondant à des conditions in situ sont se caractérisent par des déformations axiales excessives, une dilatation volumétrique et un niveau de dégradation inacceptable associé essentiellement à une cassure dans l'angle. Les résultats suggèrent que les pressions latérales in situ doivent être accrues pour compenser les charges par essieu des trains plus lourds. Des méthodes pratiques pour obtenir une augmentation du confinement sont également proposées.

INTRODUCTION

The granular layers on a railway track generally consist of an upper ballast layer composed of large, angular particles (typically 20–60 mm) and a lower layer of capping material resembling road base. The main functions of the ballast layer are to control the stress intensity projected onto the weaker subgrade, to decrease the frequency of track maintenance by minimising track settlement and sleeper movement, and to promote rapid drainage via the large pore structure. In situ lateral confining pressure results from particle interlock, sleeper resistance, residual compaction stresses, and overburden pressure, and is considerably smaller than the wheel-load-generated cyclic vertical sleeper/ballast interface pressures. This can result in significant rearrangement of particles, and the subsequent occurrence of ballast degradation, track settlement and lateral flow. Lateral spreading of particles can reduce the horizontal residual stresses that confine the layer, hence reducing the track stability (Selig & Waters, 1994). It is well established that granular materials monotonically loaded at higher confining pressures are stiffer and able to support larger loads before failure (e.g. Bishop, 1966; Charles & Watts, 1980; Indraratna *et al.*, 1998). Nevertheless, the effect of track confining pressure on substructure performance under cyclic loading has not been examined in depth.

It may be possible to enhance ballast performance by altering the level of track confinement. Indraratna *et al.* (2005) studied the degradation response of ballast under cyclic loading and determined that the degree of particle breakage is significantly affected by the magnitude of confining pressure. This study provided valuable insight into breakage behaviour, but did not provide a detailed account of the overall mechanical response. To overcome this limitation, a series of large-scale, isotropically consolidated, drained, compression, cyclic triaxial tests have been conducted and the deformation (axial and volumetric), breakage and resilient stress–strain behaviour recorded. Cyclic deviator stress amplitudes up to and exceeding the static peak

Manuscript received 26 September 2005; revised manuscript accepted 20 March 2007.
Discussion on this paper closes on 1 February 2008, for further details see p. ii.
* Douglas Partners Pty Ltd, Unanderra, Australia.
† Faculty of Engineering, University of Wollongong, Australia.
‡ Nottingham Centre for Geomechanics, School of Civil Engineering, University of Nottingham, UK.
§ RailCorp, Sydney, Australia.

strengths of the material are investigated, and the breakage theory of Indraratna *et al.* (2005) is expanded through the incorporation of additional data to include the influence of loading magnitude. The failure response of ballast to stepwise loading increments is also examined.

LABORATORY INVESTIGATIONS

Testing apparatus

The testing of coarse aggregates in conventional apparatus can give misleading results because of the disparity between particle and equipment size. As the ratio of specimen to maximum particle size approaches 6, equipment size effects can be ignored (Marachi *et al.*, 1972). Owing to the substantial physical dimensions associated with ballast, a large-scale triaxial apparatus incorporating a specimen of height 600 mm and diameter 300 mm was designed and built at the University of Wollongong. Originally intended for static or monotonic loading, the apparatus was recently upgraded with a dynamic actuator capable of deviator stresses up to 2·1 MPa and a maximum loading frequency of 60 Hz. The vertical strain is measured by recording the relative position of the actuator at regular intervals (permanent deformation) or during a given cycle (resilient deformation). A piston within the volume change device responds to water entering the (dilating) specimen or leaving the (compressing) specimen, and a linear variable differential transducer records the piston movement. Both confining pressure and back-pressure variations are recorded using transducers at the base of the specimen, and the relatively small stress distribution attributed to specimen self-weight is incorporated in the effective stresses. Further details of the apparatus components and measuring techniques can be found elsewhere (Indraratna, 1996; Indraratna *et al.*, 1998).

Material and particle size distribution

Current standards for railway ballast (e.g. Standards Australia, 1996) specify the physical and durability requirements for the parent rock, but do not evaluate performance under in situ track conditions (Chrismer, 1985). Latite basalt is commonly used as railway ballast in New South Wales, Australia, and its physical and durability attributes are shown in Table 1. Latite basalt is a dark-coloured volcanic (igneous) rock containing the main minerals feldspar, plagioclase and augite. Fig. 1(a) illustrates the particle size distribution utilised in the present study, which is representative of current industry practice (Standards Australia, 1996).

Test procedure

The latite basalt was washed and sorted into the required distribution by utilising at least two passes through a set of 13 standard sieves (aperture size 63: 2·36 mm). Specimens were then compacted to an initial density of about 1560 kg/m^3 (e_0 = 0·72–0·76) to simulate field densities for heavy haul tracks within a rubber membrane thick enough (5 mm) to prevent piercing by sharp particles during testing. Ballast specimens were saturated using a small back-pressure (15 kPa) and allowed to settle overnight. During the application of σ_3', changes in specimen volume and void ratio e were recorded, and typical changes in e during consolidation ranged from 0·05 at smaller σ_3' to 0·2 when σ_3' = 240 kPa. An initial static load was applied to each specimen at a rate of 1 mm/s to a stress equal to the average of the minimum and maximum cyclic deviator stress. A loading frequency of 20 Hz was utilised to simulate high-speed trains; nevertheless, a reduced-frequency conditioning phase (less than 5 Hz) was necessary at the commencement of cyclic loading (during rapid vertical deformation) to prevent impact loading and loss of actuator contact with the specimen. Permanent deformation data were collected at regular intervals, and bursts of data (sampling frequency = 588 Hz) were recorded at specific cycles to examine the resilient behaviour. Cyclic

Table 1. Physical and durability attributes of latite basalt (after Indraratna *et al.*, 1998)

Characteristics test results	Value	Standards Australia (1996) recommendations
Aggregate crushing value: %	12	<25
Los Angeles abrasion: %	15	<25
Wet attrition value	8	<6
Point load index: MPa	5·5	–
Compressive strength: MPa	130	–
Flakiness: %	25	<30
Misshapen particles: %	20	<30

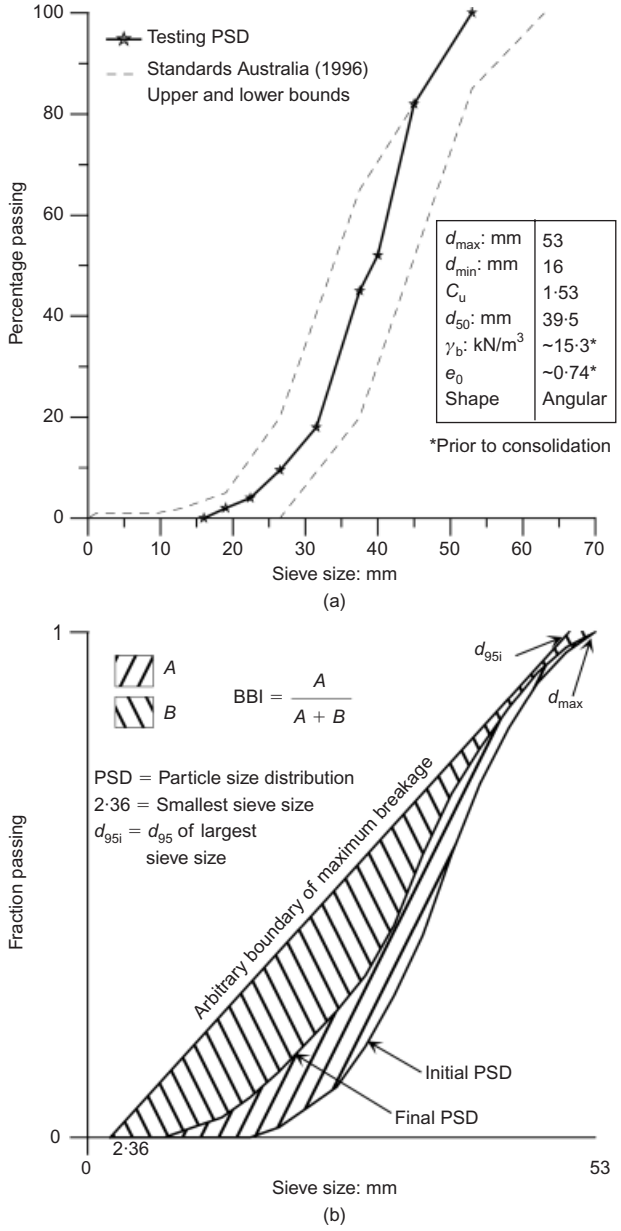

Fig. 1. Specimen characteristics and breakage quantification method: (a) initial specimen distribution, including upper and lower bounds from Standards Australia (1996); (b) ballast breakage index (BBI) calculation method (after Indraratna *et al.*, 2005)

loading continued for 500 000 cycles or until the vertical deformation reached about 25% axial strain. Upon completion of a test, the sieving procedure was repeated and the extent of breakage was evaluated. Membrane corrections were calculated using the ASTM (2002) method assuming an axial strain of 20%, a membrane thickness of 5 mm and a membrane elastic stiffness of 1100 kPa, resulting in a required correction for deviator stress of 15 kPa. This value was deemed insignificant for most specimens (<3% error), with the remaining specimens adjusted as required.

Breakage representation

Indraratna *et al.* (2005) introduced a new breakage index specifically for railway ballast to quantify the magnitude of degradation. The evaluation of the ballast breakage index (BBI) employs the change in the fraction passing a range of sieve sizes (Fig. 1(b)). By utilising a linear particle size axis, BBI can be found from equation (1), where the parameters A and B are defined in Fig. 1(b). Further details on BBI can be found in Indraratna *et al.* (2005).

$$\mathrm{BBI} = \frac{A}{A+B} \tag{1}$$

Cyclic loading conditions

The load was cycled between two compressive stress states, $q_{\mathrm{min,cyc}}$ $(\sigma'_{1\mathrm{min}} - \sigma'_3)$ and $q_{\mathrm{max,cyc}}$ $(\sigma'_{1\mathrm{max}} - \sigma'_3)$. $q_{\mathrm{min,cyc}}$ was set equal to about 45 kPa for each test, with the maximum deviator stress $q_{\mathrm{max,cyc}}$ defining the magnitude of cyclic loading. This particular $q_{\mathrm{min,cyc}}$ value was selected to represent in situ ballast layer pressures in the unloaded track state (such as sleeper and rail weights), and to prevent undesirable actuator behaviour (impact loading). σ'_1 and σ'_3 are the major and minor effective stresses respectively. The inferred radial strain ε_{r} is defined by equation (2a), where ε_{v} is the measured volumetric strain (positive in compression), and ε_{a} is the major principal strain. The mean effective stress p' is defined by equation (2b), and the resilient modulus M_{R} by equation (3), where $\varepsilon_{\mathrm{a,rec}}$ is the recoverable portion of axial strain, and Δq_{cyc} is the difference between $q_{\mathrm{max,cyc}}$ and $q_{\mathrm{min,cyc}}$. Under drained loading conditions a typical stress path has a slope of 3, and an increase in σ'_3 shifts the stress path towards higher p'.

$$\varepsilon_{\mathrm{r}} = \frac{\varepsilon_{\mathrm{v}} - \varepsilon_{\mathrm{a}}}{2} \tag{2a}$$

$$p' = \frac{\sigma_1 + 2\sigma_3}{3} \tag{2b}$$

$$M_{\mathrm{R}} = \frac{\Delta q_{\mathrm{cyc}}}{\varepsilon_{\mathrm{a,rec}}} \tag{3}$$

A total of 24 cyclic triaxial tests (Table 2) were conducted to investigate the effects of confining pressure (σ'_3), cyclic deviator stress magnitude ($q_{\mathrm{max,cyc}}$) and the number of cycles (N) on the permanent (plastic) strain, resilient modulus, and breakage of ballast. Most tests utilised cyclic amplitudes < 750 kPa to represent typical stress levels currently existing in tracks. Two tests incorporating loading magnitudes of 1000 and 1250 kPa were also included to represent the stress magnitude expected from heavier freight trains in the near future. In addition, two experiments utilised a gradually increasing loading regime to examine cyclic failure mechanisms. Values of σ'_3 ranging from 1 to 240 kPa were selected to cover the range of confining stresses that could be practically applied in situ.

EXPERIMENTAL RESULTS AND DISCUSSION

Permanent deformation behaviour

Axial and volumetric strains. During static triaxial testing of ballast it is customary for loading to continue until a certain predetermined value of axial strain ε_{a} has been obtained, for example 20%. Specimen failure is defined at the corresponding peak deviator stress $q_{\mathrm{peak,sta}} = (\sigma'_1 - \sigma'_3)_{\mathrm{peak}}$. In large granular specimens, no distinct failure plane is observed; instead, failure is usually accompanied by specimen 'bulging' (Indraratna *et al.*, 1998). During drained, stress controlled cyclic loading at constant $q_{\mathrm{max,cyc}}$, the onset of 'failure' is somewhat difficult to ascertain owing to the absence of a peak stress or a characteristic location of material weakening or softening. Failure of large ballast specimens under repeated loading is more appropriately defined by an arbitrary level of strain accumulation, such as $\varepsilon_{\mathrm{a}} \geqslant 25\%$ (corresponding to the maximum axial displacement of the dynamic actuator in the current study). Using this failure criterion, the specimens marked with an asterisk in Table 2 are said to have 'failed', with failure occurring rapidly within 500 cycles. In the absence of failure the magnitude of ε_{a} achieved at the end of a fixed number of cycles N is dependent both on the amplitudes of $q_{\mathrm{max,cyc}}$ and σ'_3, and on the breakage resistance of the particles.

Figure 2 depicts the axial strain ε_{a} and volumetric strain ε_{v} response as a function of N (for selected specimens, Figs 2(a) and 2(b)) and σ'_3 (Figs 2(c) and 2(d)). As anticipated, Fig. 2(a) indicates decreasing ε_{a} with decreasing $q_{\mathrm{max,cyc}}$ and increasing σ'_3. In concurrence with previous studies (e.g. Brown, 1974) permanent ε_{a} accumulation stabilises or shakes down within 10 000 cycles (insignificant rate of increase of ε_{a} with N). When the magnitude of stress ratio $q_{\mathrm{max,cyc}}/p'$ is sufficiently large, ε_{a} will continue to accumulate with N until $\varepsilon_{\mathrm{a}} > 25\%$. If ε_{a} remains below 25% during the initial few thousand cycles, stable shakedown conditions will prevail, albeit after significant permanent deformation in the case of specimens with relatively small σ'_3 and large $q_{\mathrm{max,cyc}}/p'$.

Reorientation and rearrangement of particles during cyclic loading generates a denser (compressing) or looser (dilating)

Table 2. Summary of triaxial tests

$q_{\mathrm{max,cyc}}$: kPa	σ'_3: kPa	Number of cycles
230	1, 10, 30, 60, 120, 240	500 000
500	3*, 10, 20, 30, 45, 60, 90, 120, 180, 240	500 000
750	30*, 60, 120, 240	500 000
1000	120	500 000
1250	120*	500 000
Increasing	60, 120	5000 cycles/interval†

*$\varepsilon_{\mathrm{a}} > 25\%$ before 500 000 cycles.
†$q_{\mathrm{max,cyc}}$ increase of 42·5 kPa/interval.

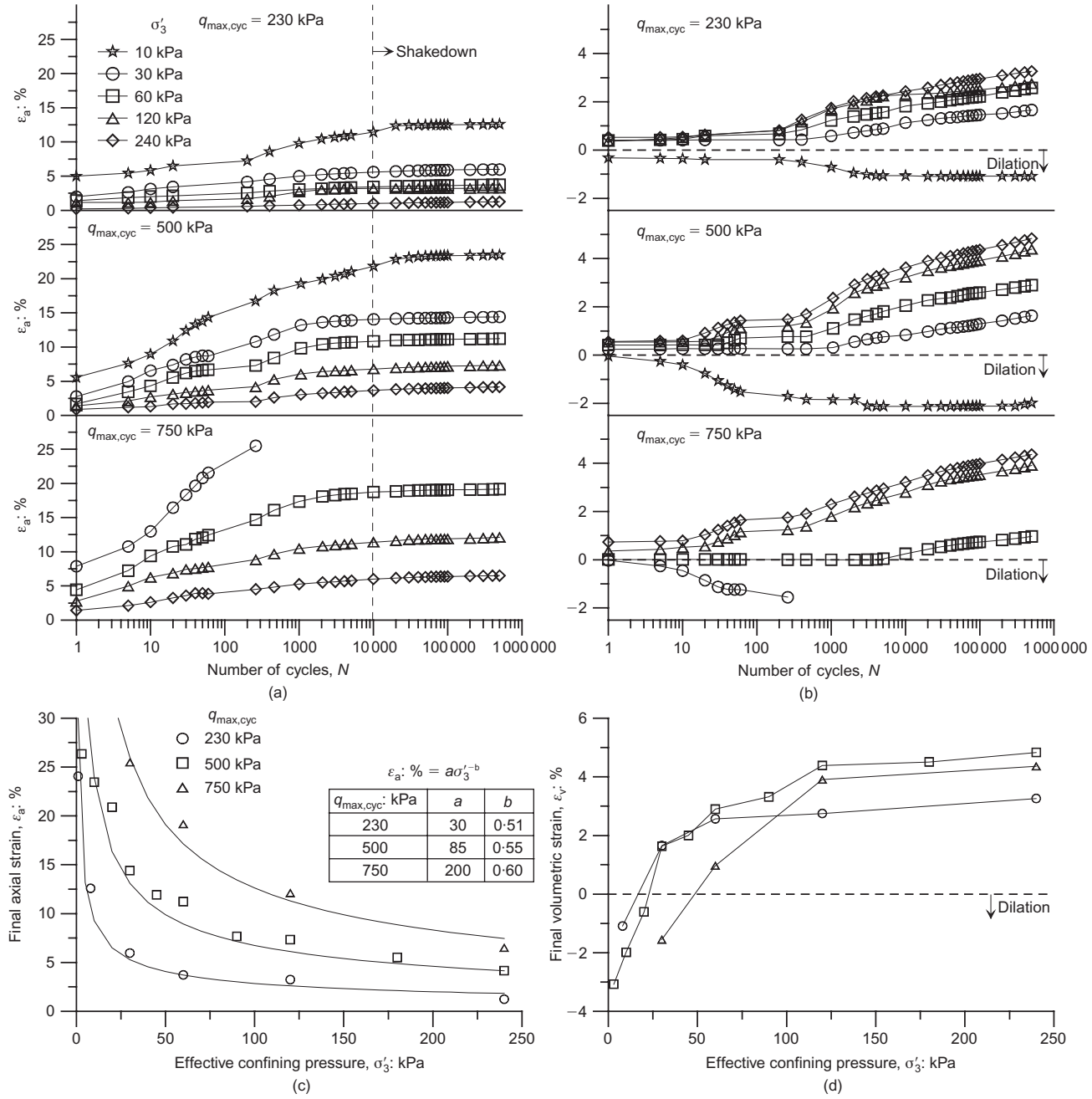

Fig. 2. Strain response under cyclic loading: (a) axial strain ε_a as a function of the number of cycles N; (b) volumetric strain ε_v as a function of N; (c) final ε_a after 500 000 cycles; (d) final ε_v after 500 000 cycles

packing assembly. Unlike ε_a, volumetric strain ε_v continues to develop at a declining rate with increasing N, as depicted in Fig. 2(b). Specimens subjected to low σ'_3 exhibit purely dilative behaviour, whereas the reverse is true for specimens with larger σ'_3. Dilation is rapid, and occurs mainly within the first 1000 cycles, and for a particular $q_{max,cyc}$, ε_v becomes more compressive with increasing σ'_3.

The effect of σ'_3 on permanent deformation of ballast is best evaluated by plotting the final values of ε_a and ε_v obtained at the completion of 500 000 cycles (Figs 2(c) and 2(d)). The dependence of ε_a on both σ'_3 and $q_{max,cyc}$ (Fig. 2(c)), and the dependence of ε_v on σ'_3 (Fig. 2(d)) are clearly apparent; however, the effect of $q_{max,cyc}$ on ε_v is not so clear. Equation (4) can be utilised to describe the influence of σ'_3 on ε_a with good correlation, where a and b are regression coefficients tabulated in Fig. 2(c).

$$\varepsilon_a(\%) = a\sigma'^{-b}_3 \tag{4}$$

Strain behaviour as a function of $q_{max,cyc}/p'$ and ψ. When considering the behaviour of granular materials under cyclic loading, it is useful to compare the magnitude of loading $q_{max,cyc}$ with the peak static deviator stress at failure, $q_{peak,sta}$, obtained from static tests. The ratio $\psi = q_{max,cyc}/q_{peak,sta}$ is hence defined for this purpose. Various researchers (e.g. Ishihara, 1985; Suiker *et al.*, 2005) have shown that, under cyclic/dynamic conditions, specimens are able to sustain significantly greater deviator stress magnitudes than statically loaded specimens: hence ψ values greater than 1 can be applied. Fig. 3 demonstrates that a bilinear relationship can accurately relate $q_{peak,sta}$ to σ'_3 for latite basalt. The depiction of the static ε_v behaviour at $q_{peak,sta}$ and $\varepsilon_a = 20\%$ in Fig. 3 also serves as a useful comparison with the cyclic ε_v response.

Figure 4 shows the axial, radial and volumetric strains after 500 000 cycles as a function of $q_{max,cyc}$ for σ'_3 values tested at different $q_{max,cyc}$ amplitudes. For a constant σ'_3,

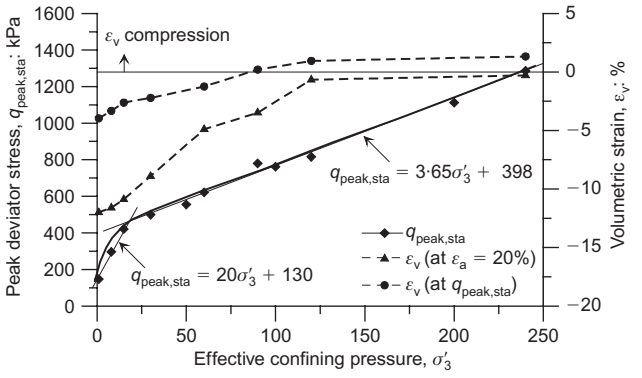

Fig. 3. Relationship between peak deviator stress at failure, $q_{peak,sta}$, and σ'_3, and volumetric strain ε_v at $q_{peak,sta}$ and ε_a = 20% (after Indraratna *et al.*, 1998, and Salim, 2004)

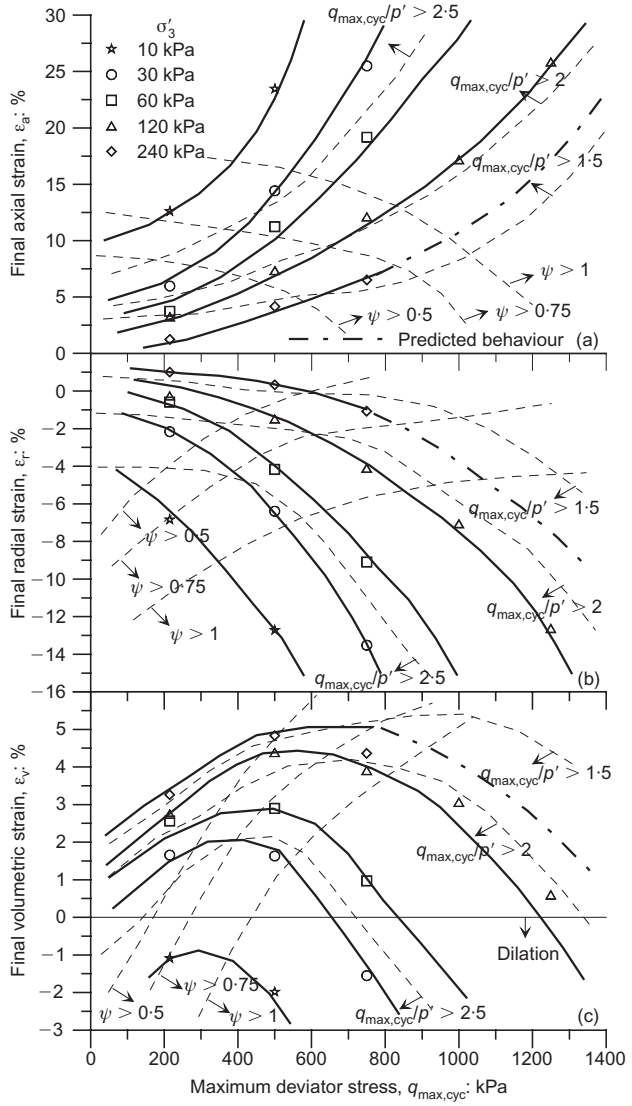

Fig. 4. Final strain values after 500 000 cycles and ψ and $q_{max,cyc}/p'$ contours as a function of $q_{max,cyc}$ for: (a) axial strain ε_a; (b) radial strain ε_r; (c) volumetric strain ε_v

increasing ψ and $q_{max,cyc}/p'$ generates larger axial (Fig. 4(a)) and radial (Fig. 4(b)) strains. Fig. 4(c) shows that volumetric straining tendencies are dependent on both ψ and σ'_3, and that ε_v becomes more dilative with increasing $q_{max,cyc}/p'$. Raymond and Williams (1978) subjected specimens of Coteau dolomite ballast to ψ ratios ranging from 0·25 to 0·75 and witnessed increasing ε_v with ψ for σ'_3 = 206·8 kPa, signifying a point of maximum specimen compression at $\psi > 0{\cdot}75$. Negligible difference in ε_v was encountered for $\psi = 0{\cdot}5$ and 0·75 when σ'_3 was decreased to 51·7 kPa. In the current study, specimens display compressive behaviour when $\psi < 0{\cdot}5$, and the magnitude of compression increases with $q_{max,cyc}$ and σ'_3. However, as ψ increases beyond 0·5, ε_v peaks and then starts to decline as $\psi = 1$ is approached (Fig. 4(c)), suggesting a point of maximum compression at $\psi \approx 0{\cdot}75$. With continued increases in $q_{max,cyc}$ specimen compression declines, until $\psi \gg 1$ and all specimens dilate upon loading. The $q_{max,cyc}$ required to instigate maximum compression increases with σ'_3. For the condition $\psi > 1$, Fig. 4(c) shows that the incidence of dilative behaviour increases with decreasing σ'_3. Compared with static loading (Fig. 3), cyclically loaded specimens display a significantly higher tendency for rapid initial compression, although this effect may diminish with increasing initial density. Suiker *et al.* (2005) showed that granular materials display a strong tendency to compact under cyclic loading, even as ψ approaches 1, and a similar behaviour is observed in the current study.

Given ψ or $q_{max,cyc}$, it is possible to predict ε_a after 500 000 cycles for latite basalt using Fig. 5. Irrespective of the applied stresses, the variation of ε_a is confined within a narrow band when plotted against ψ for $\psi \leqslant 2$. A best-fit median equation for the data shown in Fig. 5 can be presented as

$$\varepsilon_a(\%) = \alpha + \beta\psi \tag{5}$$

For a good positive regression ($R^2 > 0{\cdot}98$), α and β are material constants equal to -3 and 18 respectively.

Resilient deformation. The effect of σ'_3 and $q_{max,cyc}$ on the resilient modulus M_R was assessed by recording the resilient (recoverable) strain $\varepsilon_{a,rec}$ and deviator stress magnitude Δq_{cyc} at numerous cycles N throughout each test. Previous research (e.g. Allen, 1973; Khedr, 1985) recognised that M_R is independent of N after the completion of a small number of stress repetitions (typically less than 1000 cycles). Fig. 6(a), however, shows a continuing increase in M_R with N, although little change is observed beyond 100 000 cycles. Selig & Alva-Hurtado (1982) recognised that a reduction in $\varepsilon_{a,rec}$ with each successive cycle and subsequent increase in M_R can be attributed, at least partly, to densification from cumulative ε_v. As ε_v increases indefinitely with N (Fig. 2(b)), leading to a reduction in void ratio and thus increased specimen stiffness, the progression of M_R with N in Fig. 6(a) is warranted. Fig. 6(a) also shows an increase in M_R with σ'_3, which has been reported previously in the literature (Hicks, 1970; Allen, 1973). The effect of $q_{max,cyc}$ (or Δq_{cyc}) on M_R is depicted in Fig. 6(b) as a function of N, and in Fig. 6(c) as a function of

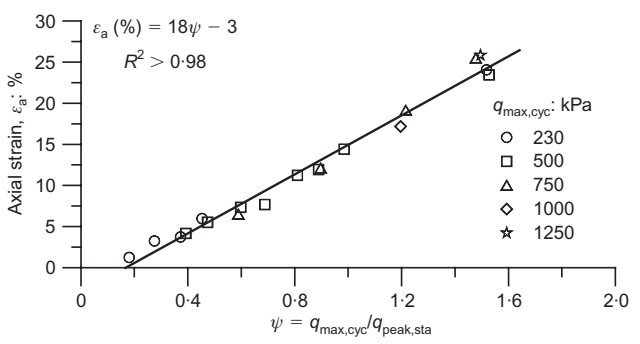

Fig. 5. Prediction of final axial strain ε_a after 500 000 cycles based on ratio ψ

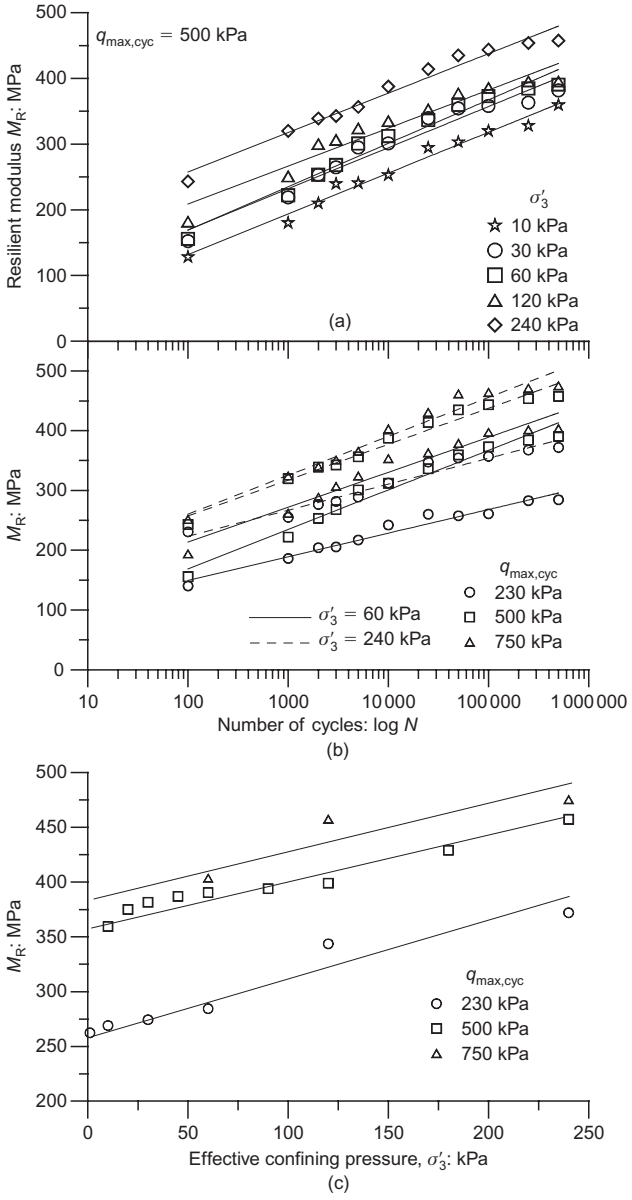

Fig. 6. Resilient modulus M_R response under various stress states: (a) effect of confining pressure σ'_3 and number of cycles N on M_R for $q_{max,cyc}$ = 500 kPa; (b) effect of $q_{max,cyc}$ on M_R for σ'_3 = 60 and 240 kPa; (c) final M_R achieved after 500 000 cycles

σ'_3. It is shown that the magnitude of M_R increases with $q_{max,cyc}$, and this may be due to the corresponding increase in mean normal effective stress associated with increasing $q_{max,cyc}$.

These results clearly show that a higher magnitude of confinement is beneficial in minimising the permanent and resilient deformation of tracks. It would therefore seem appropriate to maximise the lateral constraint on the in situ ballast layer. The extent of particle degradation, however, may be affected by the degree of confining stress. Degradation results in reduced particle size and angularity, and a subsequent decline in the overall shear strength and drainage capability of the ballast layer. The breakage behaviour has consequently been examined with the intention of relating σ'_3 and $q_{max,cyc}$ to the expected degree of degradation.

Cyclic degradation behaviour

Lees & Kennedy (1975) recognised that the degradation of granular materials can occur in three ways:

(*a*) the breakage of angular corners or projections
(*b*) the grinding or attrition of asperities
(*c*) the splitting of particles into two or more approximately equal parts.

The fracture (splitting) probability of a particle subjected to compressional forces within a granular medium is a function of the applied stresses ($q_{max,cyc}$ and σ'_3), the particle size, and the coordination number, that is, the number of particle contacts (McDowell *et al.*, 1996; McDowell & Bolton, 1998). Owing to the angular nature of ballast, however, Indraratna *et al.* (2005) showed that most ballast degradation is not attributable to particle splitting, but is instead primarily the consequence of corner breakage.

Indraratna *et al.* (2005) established that ballast degradation behaviour under cyclic loading can be categorised into three distinct zones: the dilatant unstable degradation zone (DUDZ), the optimum degradation zone (ODZ), and the compressive stable degradation zone (CSDZ). These zones were initially defined by the level of σ'_3 acting on the specimen (i.e. DUDZ, $\sigma'_3 < 30$ kPa; ODZ, 30 kPa $< \sigma'_3 <$ 75 kPa; CSDZ, $\sigma'_3 > 75$ kPa); however, $q_{max,cyc}$ also plays an important role in characterising the zones, as explained below.

Dilatant unstable degradation zone (DUDZ). Specimens that are subjected to low σ'_3, and which experience overall volumetric dilation caused by rapid and considerable axial and expansive radial strains, are characterised in the DUDZ (Fig. 7). Degradation in the DUDZ is considered the most significant of the three zones, with breakage occurring predominantly at the onset of loading, when the axial strain and dilation rates are at a maximum. The micromechanical processes responsible for degradation in the DUDZ have been briefly described in Indraratna *et al.* (2005). However, further examination is warranted, owing to the possible implications associated with low in situ confining pressures. Oda (1972) and Cundall *et al.* (1982) ascertained that the deviatoric force in a granular material is transmitted mainly through chain- or column-like structures aligned in the direction of the major principal stress. Consider, for example, a DUDZ ballast specimen with major principal stress σ'_1 equal to 780 kPa (macroscopic $q_{max,cyc}$ = 750 kPa, σ'_3 = 30 kPa) with diameter 300 mm. This translates to an axial force F of 55 kN, which might be distributed over, say, four ballast columns, so that the induced characteristic stress (defined as F/d^2) on a ballast particle of diameter d = 40 mm would be about 8·5 MPa. This stress may not be sufficient to cause splitting of the particle, based on the particle strengths given by Lim *et al.* (2005). However, if the characteristic stress F/a^2 induced in a small angular projection of size a in a deforming ballast column is considered, it is very likely to fracture. Most of the degradation in this zone is due to the breakage of angular corners or projections, and very little particle splitting is observed. The lack of particle splitting is due to internal deformation mechanisms, such as sliding or rolling, that inhibit the formation of permanent interparticle contacts, thus preventing splitting due to excessive stresses.

For relatively minor $q_{max,cyc}$ such as 230 kPa (Fig. 7(d)), the DUDZ σ'_3 range is comparatively small because the $q_{max,cyc}$ magnitude is insufficient to cause dilation, a main requirement for DUDZ behaviour. As the deviator stress $q_{max,cyc}$ increases (Figs 7(c) and 7(b)), the tendency for dilation is much greater: thus the σ'_3 range of the DUDZ increases. The upper σ'_3 DUDZ boundaries for each respective $q_{max,cyc}$ are tabulated in Fig. 7(d), and can be determined from Fig. 2(d) at $\varepsilon_v = 0$. DUDZ degradation can be avoided for latite basalt if σ'_3 values greater than 15, 25 or

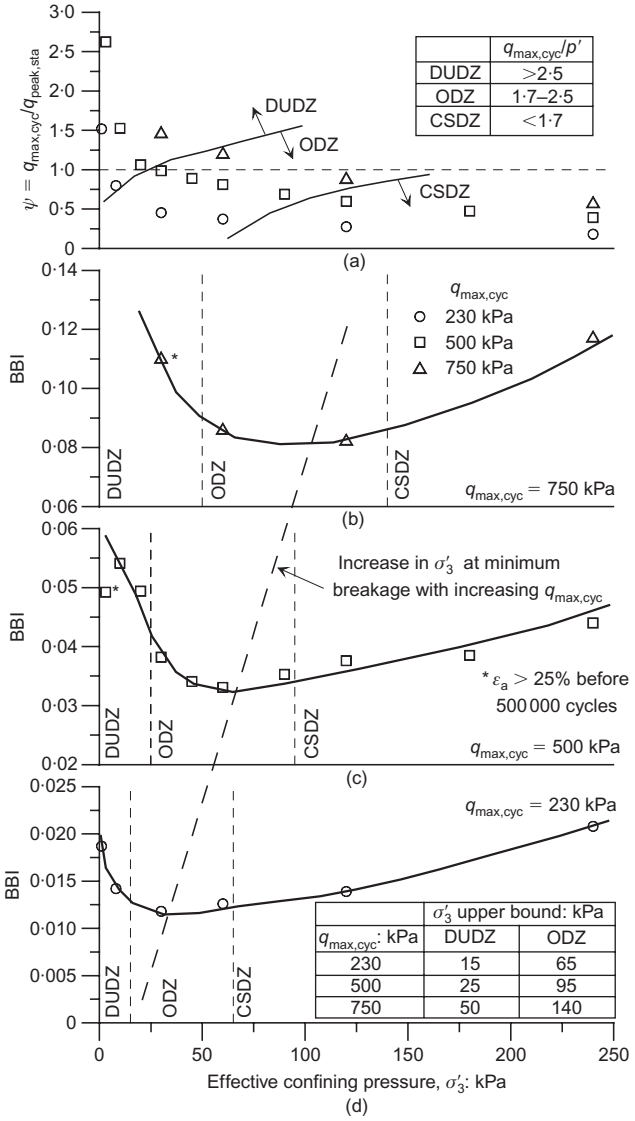

Fig. 7. Effect of confining pressure σ'_3 and maximum deviator stress $q_{max,cyc}$ on ballast breakage index BBI, and effect of $q_{max,cyc}$ on DUDZ, ODZ and CSDZ breakage zones

50 kPa are applied for $q_{max,cyc}$ = 230, 500 and 750 kPa respectively.

Figure 7(a) shows that most specimens in the DUDZ were subjected to ψ values >1. Therefore it appears that the three basic requirements for DUDZ behaviour are a small σ'_3, specimen dilation, and $\psi > 1$. Undoubtedly, the DUDZ conditions should be avoided on railway tracks as much as possible.

Optimum degradation zone (ODZ). Similar to the DUDZ, the range of σ'_3 defining the ODZ is influenced by the applied $q_{max,cyc}$, as indicated in Fig. 7. Indraratna *et al.* (2005) showed that a small increase in σ'_3 is sufficient to cause an optimum internal contact stress distribution and increased interparticle contact areas, resulting in diminished tensile stresses within particles and hence significantly reduced breakage, lower axial strains, and overall specimen compression. Oda (1977) correlated decreasing void ratio with increasing coordination number: therefore the coordination number is expected to be slightly increased (compared with DUDZ specimens) owing to the reversal of ε_v behaviour (from dilation to compression).

From Fig. 7(a) it can be perceived that ODZ specimens generally have ψ values ranging from about 0·4 up to 1·2. Increasing the magnitude of $q_{max,cyc}$ also results in a wider ODZ zone (Fig. 7(d)), with the ODZ defined as 15–65 kPa, 25–95 kPa and 50–140 kPa for $q_{max,cyc}$ = 230, 500 and 750 kPa respectively.

Compressive stable degradation zone (CSDZ). In the CSDZ, particle movement and dilation are largely suppressed owing to the considerable levels of confinement, as explained in Indraratna *et al.* (2005). The σ'_3 boundary between the ODZ and CSDZ can be defined by a 'flattening out' of ε_v in Fig. 2(d). The most significant differences between the ODZ and CSDZ are the reduced mobility of particles and the highly stressed but relatively secure contact points. Although corner degradation is still the foremost kind of breakage, some particle splitting takes place through planes of weakness such as microcracks and other flaws, and the fatigue of particles becomes more prominent in the CSDZ (Indraratna *et al.*, 2005). The vertical force chains are expected to be less vertical and more isotropic owing to lateral resistance from surrounding particles. Irrespective of the lower ψ ratios in the CSDZ, breakage is more significant in this zone than in the ODZ. CSDZ conditions are encountered when $\sigma'_3 > 65$, 95 and 140 kPa for $q_{max,cyc}$ = 230, 500 and 750 kPa respectively.

In essence, Fig. 7 shows that the confining pressure responsible for minimum breakage increases with the loading amplitude. Alternatively, if railway organisations were to increase train axle loads, an increased ballast confinement would be required to reduce ballast degradation. Fig. 8(a) shows the relative particle size distribution curves for speci-

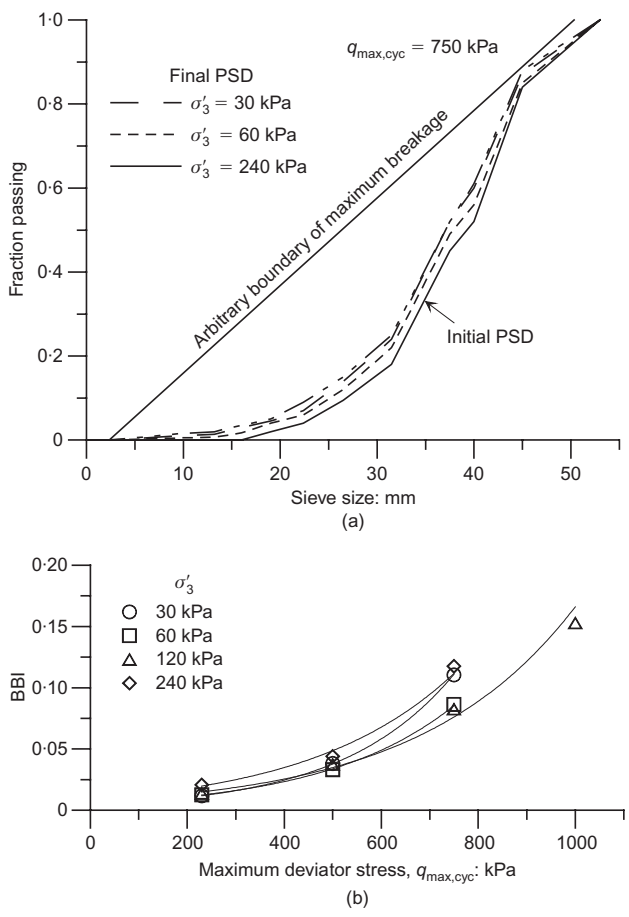

Fig. 8. (a) Relative particle size distribution curves after loading for a DUDZ, ODZ and CSDZ specimen ($q_{max,cyc}$ = 750 kPa, σ'_3 = 30, 60 and 240 kPa respectively); (b) effect of maximum cyclic deviator stress $q_{max,cyc}$ on ballast breakage index BBI

mens in each zone ($q_{max,cyc} = 750$ kPa and $\sigma'_3 = 30$, 60 and 240 kPa) in terms of the calculation of BBI. The effect of $q_{max,cyc}$ on the breakage behaviour of ballast is depicted in Fig. 8(b), and it appears that a non-linear relationship exists between $q_{max,cyc}$ and BBI.

Cyclic failure under stepwise loading

In the preceding sections an arbitrary value of strain accumulation ($\varepsilon_a \geqslant 25\%$) was considered to define specimen failure under constant $q_{max,cyc}$ cyclic loading. Failure occurred rapidly within 500 cycles, usually not allowing sufficient time for the evaluation of specimen response during or just after the onset of failure. To overcome this limitation, two cyclic triaxial tests (see Table 2) were conducted wherein the cyclic deviator stress $q_{max,cyc}$ was gradually increased in a stepwise fashion (Fig. 9(a)) until $\varepsilon_a \geqslant 20\%$ (to correspond to the static failure conditions of Indraratna *et al.*, 1998, and Salim, 2004). Although the loading regime chosen in Fig. 9 is arbitrary, and unlikely to be encountered in practice, it nevertheless illustrates cyclic densification of ballast and demonstrates the reduction in track bed stability with increasing $q_{max,cyc}$. The tests have been limited to one loading regime ($N = 5000$ cycles per

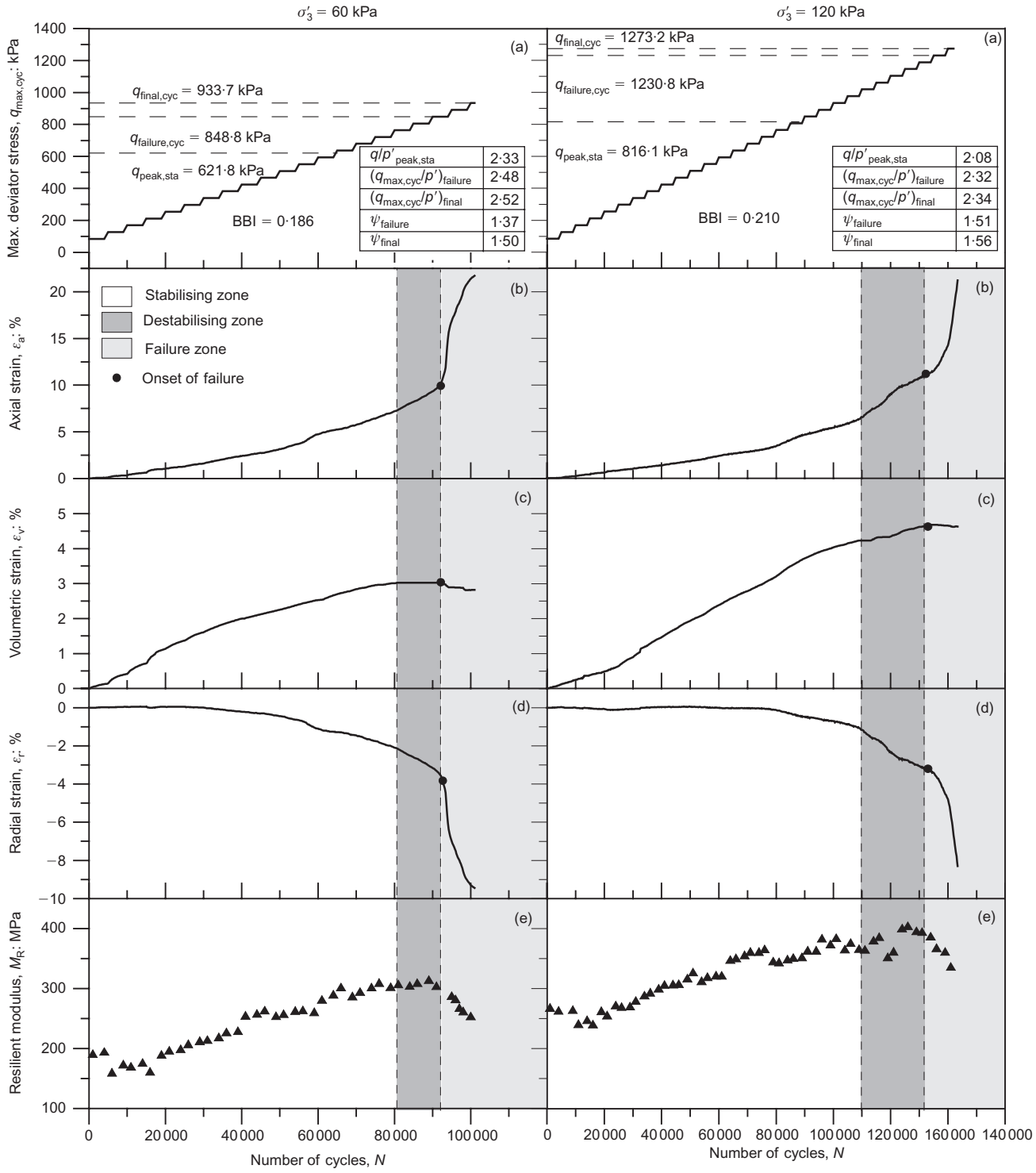

Fig. 9. Behaviour of ballast under stepwise loading: (a) loading regime; (b) axial strain ε_a; (c) volumetric strain ε_v; (d) radial strain ε_r; (e) resilient modulus M_R

interval and increasing $q_{max,cyc}$ of 42·5 kPa per interval), and it is acknowledged that changes in these parameters may affect the results.

Figure 9 shows that stepwise cyclic loading presents a distinctly different form of failure from constant-$q_{max,cyc}$ loading. 'Failure' (marked with a black dot) is characterised by a sudden increase in axial strain (Fig. 9(b)) but only a marginally changing volumetric strain (Fig. 9(c)), plus a significant decrease in the resilient modulus (Fig. 9(d)). Before the commencement of failure, Fig. 9 demonstrates a stabilising zone followed by a period of destabilisation.

Compared with static triaxial testing (Fig. 3), the extent of dilation at failure under stepwise cyclic loading is relatively insignificant, highlighting the greater compression tendencies of cyclically loaded specimens. Fig. 9(a) also demonstrates that specimens under cyclic loading fail at $q_{max,cyc}$ significantly greater than $q_{peak,sta}$ (ψ at failure = 1·37 and 1·51 for σ_3' = 60 and 120 kPa respectively), signifying significant material strength development in the stabilising zone.

PRACTICAL IMPLICATIONS

From the previous discussions it is apparent that effective confining pressure has a significant influence on the cyclic behaviour of railway ballast, and should therefore be considered in the design of railway foundations. Increased confinement would result in decreased track settlement and greater track stability and stiffness (resilient modulus) under cyclic loading, leading to greater ride comfort. Enhancement of the lateral track confinement could be achieved conceptually by

(*a*) increasing the degree of particle interlock or ballast friction angle
(*b*) preventing lateral ballast flow using containing sheets (restraints) at the shoulders (Fig. 10(a)) or geosynthetics at the ballast/capping interface
(*c*) redesigning the sleeper shape to reduce ballast flow (winged precast concrete sleepers, Fig. 10(b)), or
(*d*) increasing the shoulder height, and/or further compaction of the shoulder and crib ballast.

A field trial is currently being conducted in Bulli (near Wollongong in NSW, Australia) to validate the merits of these methods.

CONCLUSIONS

Few substructure modifications have been made in recent years to compensate for increasing freight. The possibility of modifying track confining pressure as a potential means of substructure enhancement has been explored using a series of large-scale drained, cyclic triaxial tests. Results of this study confirm that the confining pressure should be considered as an important design parameter.

The magnitude of vertical (axial) strain ε_a was found to be a function of the applied deviator stress $q_{max,cyc}$ and the degree of lateral confinement σ_3', with shakedown shown to occur within 10 000 cycles. The degree of volumetric compression ε_v increased indefinitely with N and σ_3' for constant $q_{max,cyc}$. Overall specimen volumetric compression increased for ψ ratios ($\psi = q_{max,cyc}/q_{peak,sta}$) up to about 0·75, and beyond this value the ballast behaviour became increasingly dilatant.

The ballast degradation response was characterised into three zones depending on the magnitudes of σ_3' and $q_{max,cyc}$. The highly dilatant behaviour in the DUDZ ($q_{max,cyc}/p' > 2{\cdot}5$) at low σ_3' was acknowledged as unfavourable in relation to permanent deformation and particle degradation, and should therefore be avoided in-track. Optimal breakage conditions were established in the ODZ ($1{\cdot}7 < q_{max,cyc}/p' < 2{\cdot}5$) within the σ_3' ranges of 15–65 kPa, 25–95 kPa and 50–140 kPa, for $q_{max,cyc}$ magnitudes of 230, 500 and 750 kPa respectively, indicating that future increases in train load require a corresponding increase in track confinement if particle degradation is to be minimised. Ballast subjected to stepwise cyclic loading exhibits rapid axial and radial strains at failure, but less dilation than monotonically loaded specimens, and a decline in resilient modulus. Specimens undergoing such stepwise loading failed at ψ equal to 1·37 and 1·51 for σ_3' = 60 and 120 kPa respectively, indicating that cyclic loading can enhance the peak strength of ballast.

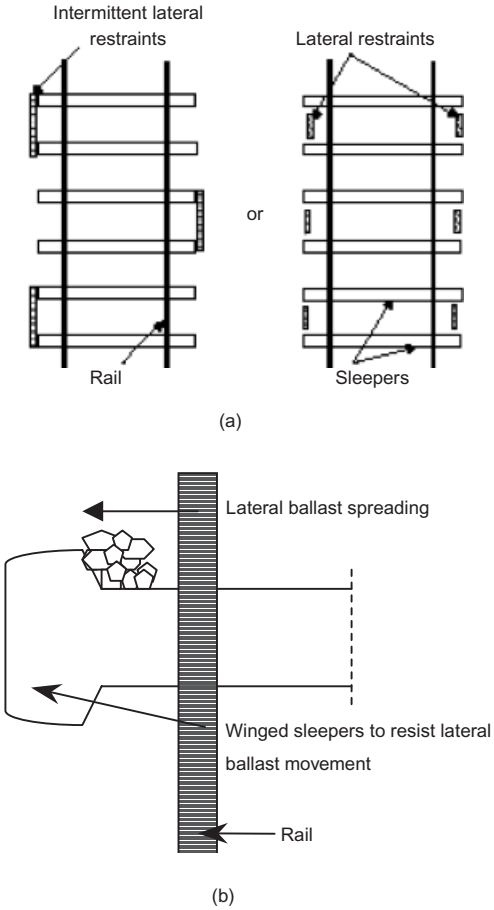

Fig. 10. Potential methods of increasing confining pressure using: (a) intermittent lateral restraints (after Indraratna *et al.*, 2004); (b) winged sleepers

This study shows that simple substructure design alterations can be implemented in-track to improve the performance of the entire track system and reduce the need for costly maintenance. Large-scale triaxial tests on ballast have indicated that increasing the degree of lateral confining pressure in the railway substructure by a small degree should be beneficial in increasing track stability. The level of lateral confinement is a fundamental design criterion for many geotechnical applications, but currently no standards exist in relation to lateral ballast confinement in rail tracks. If an appropriate confining pressure is implemented for local in situ conditions, rail tracks can be improved in terms of degradation and deformation resistance, with enhanced resilience characteristics.

NOTATION

a, b, c, d	regression coefficients
BBI	ballast breakage index
C_u	coefficient of uniformity
e	void ratio

e_0	initial void ratio
M_R	resilient modulus (MPa)
N	number of cycles
$q_{failure,cyc}$	cyclic deviator stress at failure during stepwise tests
$q_{final,cyc}$	cyclic deviator stress at $\varepsilon_a = 20\%$ during stepwise tests
$q_{max,cyc}$	maximum deviator stress magnitude
$q_{min,cyc}$	minimum deviator stress magnitude
$q_{peak,sta}$	maximum static peak deviator stress
p'	mean effective stress
Δq_{cyc}	$q_{max,cyc} - q_{min,cyc}$
α, β	regression coefficients
γ_b	bulk unit weight
ε_a	axial strain
$\varepsilon_{a,rec}$	recoverable portion of axial strain
ε_r	radial strain
ε_v	volumetric strain
ψ	$q_{max,cyc}/q_{peak,sta}$
σ'_1	major principal stress
σ'_3	effective confining pressure

REFERENCES

Allen, J. J. (1973). The effects of non-constant lateral pressures on the resilient properties of granular materials. PhD thesis, University of Illinois.

ASTM (2002). *Standard test method for consolidated undrained triaxial compression test for cohesive soils*, ASTM D4767-02. West Conshohocken, PA: ASTM International.

Bishop, A. W. (1966). The strength of soils as engineering materials. *Géotechnique* **16**, No. 2, 91–128.

Brown, S. F. (1974). Repeated load testing of a granular material. *J. Geotech. Engng Div. ASCE* **100**, No. GT7, 825–841.

Charles, J. A. & Watts, K. S. (1980). The influence of confining pressure on the shear strength of compacted rockfill. *Géotechnique* **30**, No. 4, 353–367.

Chrismer, S. M. (1985). *Considerations of factors affecting ballast performance*, AREA Bulletin AAR Research and Test Dept. Chicago: AAR Technical Centre. Report No. WP-110, pp. 118–150.

Cundall, P. A., Drescher, A. & Strack, O. D. L. (1982). Numerical experiments on granular assemblies: measurements and observations. *Proceedings of the IUTAM conference on deformation and failure of granular materials*, Delft, pp. 355–370.

Hicks, R. G. (1970). *Factors influencing the resilient properties of granular materials*. PhD thesis, University of California.

Indraratna, B. (1996). Large-scale triaxial facility for testing non-homogeneous materials including rockfill and railway ballast. *Aust. Geomech.* **30**, December, 125–126.

Indraratna, B., Ionescu, D. & Christie, H. D. (1998). Shear behavior of railway ballast based on large-scale triaxial tests. *J. Geotech. Geoenviron. Engng* **124**, No. 5, 439–449.

Indraratna, B., Khabbaz, H., Salim, W. & Lackenby, J. (2004). Ballast characteristics and the effect of geosynthetics on rail track deformation. *Proceedings of the international conference on geosynthetics and geoenvironmental engineering*, Bombay, 3–13.

Indraratna, B., Lackenby, J. & Christie, D. (2005). Effect of confining pressure on the degradation of ballast under cyclic loading. *Géotechnique* **55**, No. 4, 325–328.

Ishihara, K. (1985). Stability of natural deposits during earthquakes. *Proc. 11th Int. Conf. Soil Mech. Found. Engng, San Francisco*, **2**, 321–376.

Khedr, S. (1985). Deformation characteristics of granular base course in flexible pavements. *Transp. Res. Rec.*, No. 1043, 131–138.

Lees, G. & Kennedy, C. K. (1975). Quality, shape and degradation of aggregates. *J. Engng Geol.* **8**, No. 3, 193–209.

Lim, W. L., McDowell, G. R. & Collop, A. C. (2005). Quantifying the relative strengths of railway ballasts. *Proc. Instn Civ. Engrs, Geotech. Engng* **158**, No. GE2, 107–111.

Marachi, N. D., Chan, C. K. & Seed, H. B. (1972). Evaluation of properties of rockfill materials. *J. Soil Mech. Found. Div. ASCE* **98**, No. 1, 95–114.

McDowell, G. R. & Bolton, M. D. (1998). On the micromechanics of crushable aggregates. *Géotechnique* **48**, No. 5, 667–679.

McDowell, G. R., Bolton, M. D. & Robertson, D. (1996). The fractal crushing of granular materials. *J. Mech. Phys. Solids* **44**, No. 12, 2079–2102.

Oda, M. (1972). Deformation mechanism of sand in triaxial compression tests. *Soils Found.* **12**, No. 4, 45–63.

Oda, M. (1977). Co-ordination number and its relation to shear strength of granular material. *Soils Found.* **17**, No. 2, 29–42.

Raymond, G. P. & Williams, D. R. (1978). Repeated load triaxial tests on dolomite ballast. *J. Geotech. Engng Div. ASCE* **104**, No. GT7, 1013–1029.

Salim, W. M. D. (2004). *Deformation and degradation aspects of ballast and the role of geosynthetics in track stabilisation*. PhD thesis, University of Wollongong.

Selig, E. T. & Alva-Hurtado, J. E. (1982). Predicting effects of repeated wheel loading on track settlement. *Proc. 2nd Int. Heavy Haul Railway Conf.*, Colorado Springs, 476–487.

Selig, E. T. & Waters, J. M. (1994). *Track geotechnology and substructure management*. London: Thomas Telford.

Standards Australia (1996). *Aggregates and rock for engineering purposes*, AS 2758·7-1996. Sydney: Standards Australia.

Suiker, A. S. J., Selig, E. T. & Frenkel, R. (2005). Static and cyclic triaxial testing of ballast and subballast. *J. Geotech. Geoenviron. Engng ASCE* **131**, No. 6, 771–782.